

A Greedy Quantum Route-Generation Algorithm

Jordan Makansi

*Department of Civil and Environmental Engineering
University of Southern California
Los Angeles, 90007 CA
makansi@usc.edu*

Abstract—Routing and scheduling problems with time windows have long been important optimization problems for logistics and planning. Many classical heuristics and exact methods exist for such problems. However, there are no satisfactory methods for generating routes using quantum computing (QC), for mainly two reasons: inequality constraints, and the trade-off of feasibility and solution quality. Inequality constraints are typically handled using slack variables; and feasible solutions are found by filtering samples. These challenges are amplified in the presence of noise inherent in QC. Here, we propose a greedy algorithm that generates routes by using information from all samples obtained from the quantum computer. By noticing the relationship between qubits in our formulation as a directed acyclic graph (DAG), we designed an algorithm that adaptively constructs a feasible solution. We prove its convergence to a feasible solution, and illustrate its efficacy by solving the Fleet Sizing Vehicle Routing Problem with Time Windows (FSVRPTW). Our computational results show that this method obtains a lower objective value than the current state-of-the-art annealing approaches, both classical and hybrid, for the same amount of time using D-Wave’s Hybrid Solvers. We also show its robustness to noise on D-Wave’s Advantage 4.1 through computational results as compared to the filtering approach on DWaveSampler, even when the filtering approach is given a longer annealing time, and a larger sample size.

Index Terms—QUBO, quantum annealing, VRP, routing, greedy, D-Wave.

I. INTRODUCTION

One of the most important problems in operations research is servicing customers within a certain time window. The simplest version of this is the travelling salesman problem with time windows, but more complex versions of this problem have also become relevant as transportation and logistics problems have become more complex. In this paper we study the Fleet Size Vehicle Routing Problem with Time Windows (FSVRPTW), which determines the minimum number of vehicles required to service all customers within their respective time windows.

The problem is practically-relevant on its own, but it is also a sub-problem in many solution methods for more complex routing problems such as column generation, bender’s decomposition, branch-and-price. However, in the aforementioned solution approaches, an exact solution method to the sub-problem is not always necessary - but a computationally-tractable one, is. Therefore, the community would benefit from faster solutions to this problem.

This research was supported in part by the PWICE institute at USC.

Quantum computing (QC) offers exciting possibilities to perform certain computational tasks better than classical solvers and may be able to speed up challenging optimization problems such as route planning. Certain algorithms such as Shor’s factorization or Grover’s search have proven advantage over their classical counterparts in fault-tolerant conditions. In the near future, it is not certain whether a quantum advantage can be observed due to the noise, and current size capabilities of quantum computers. As such, many hybrid approaches, involving classical and quantum computing, have been proposed. However, it still remains relevant to determine the best quantum approach to certain problems, so that when the QC capabilities become more advanced, the solution methods are readily available.

Routing problems on quantum computers have been solved since Feld et al [1]. However, no annealing-based methods have shown to be practical for generating routes themselves. Existing approaches that have shown to be capable of solving problems at scale generate routes classically, and then solve a set cover or exact cover problem. On the other hand, the existing annealing-based approaches do not scale well, due to slack variables, and other inefficient encoding schemes [2]. We review them briefly: [3] solves the traveling salesperson problem with time windows (TSPTW) using slack variables and one-hot encoding. This makes the number of qubits impractical. [4] uses position-based indexing. While this works under the single-agent setting in TSPTW, it loses much in optimality in a multi-agent setting because it assumes each agent makes a maximum number of stops. [5] creatively discretizes time using a state-based description, but the formulation of time-windows has a discrepancy with the capacity and state description. [6] presents several QUBO formulations but only solves small-sized problems, and, aside from the route-based formulation has difficulty obtaining feasible solutions. [7], [8] and [9] all present creative hybrid solution methods, but still generate routes classically.

The majority of existing QC solutions to Sherrington-Kirkpatrick (SK) Ising models involve sampling the QC a number of times, and eventually selecting the sample with the lowest energy. However, emerging research has shown the potential to use all of the samples from the QC, to take advantage of the correlation between samples [10]. We review them briefly here. [11] uses an iterative approach that fixes qubits based on their one-body expectation value, computed by using all of the samples returned from the annealer. Qubits

with expectation values above a certain threshold are fixed to a particular value based on a majority vote, and a smaller SK Ising model is solved at the next iteration. The expectation value in some sense measures how certain we are of its value. [12], unlike [11], this paper has two separate procedures for selecting which qubits to fix, and the values they are fixed to. After selecting qubits, their values are determined by brute-force evaluation of the expectation value of the objective function, over all possible values of the selected variables. [13] uses two phases, instead of an iterative approach: 1) Run QAOA. 2) Compute the correlation matrix given by the output from sampling the QC circuit constructed from QAOA. The values of the principal eigenvector are then rounded to obtain a final solution. Other efforts to improve solution quality, e.g. unbalanced penalization [14], still cannot guarantee a feasible solution, and require heavy classical pre-processing for tuning penalty parameters. They also do not disclose computation time in their computational results.

However, these approaches do not directly apply to solve constrained optimization problems; the process of fixing variables may decrease the expectation value of the energy, but it might also violate constraints. The fixed values are maintained permanently throughout the remainder of the algorithm. For constrained problems, we require a delicate approach for ensuring a feasible solution can still be returned after the variables are fixed. We propose an algorithm which takes advantage of both the emerging research to utilize the correlation between samples, and also is guaranteed to return a feasible solution to the FSVRPTW. In this paper we present an annealing-based algorithm for generating routes under time window constraints that is suitable for the NISQ era [15] by its convergence to a feasible solution, and competitive computation time and solution quality. Our main contributions are as follows:

- Present an annealing-based algorithm for generating routes, that represents the samples returned by the annealer as a DAG.
- Prove that it converges to a feasible solution.
- Show computational results on D-Wave, benchmarking it against classical, hybrid, and quantum annealing-based approaches based on computation time, and optimality, for a variety of practical-sized benchmark instances.

II. PRELIMINARIES

A. Quadratic Unconstrained Binary Optimization

Many discrete optimization problems can be formulated as a Quadratic Unconstrained Binary Optimization (QUBO) problem. It is the common format used to input optimization problems into quantum annealers. Given square matrix $Q \in \mathbb{R}^{n \times n}$, the problem is to minimize $x^T Q x$ over binary variables $x_i \in \{0, 1\}^n$:

$$\min_{x \in \{0, 1\}^n} x^T Q x \quad (1)$$

Coefficients for linear terms in an optimization problem may be represented in the QUBO form by the diagonal elements

TABLE I: Timetable and distance matrix

| Timetable | | | | Distance Matrix | | | | |
|-----------|-------|----------|-------|-----------------|---|---|---|---|
| i | e_i | l_i | q_i | i | 0 | 1 | 2 | N |
| 0 | 0.0 | ∞ | 0.0 | 0 | 0 | 1 | 3 | 0 |
| 1 | 1.0 | 1.15 | 1.0 | 1 | 1 | 0 | 2 | 1 |
| 2 | 3.5 | 3.75 | 1.0 | 2 | 3 | 2 | 0 | 3 |
| N | 0.0 | ∞ | 0.0 | N | 0 | 1 | 3 | 0 |

of the matrix Q , since $x_i^2 = x_i$. To represent this optimization problem on a quantum device, the QUBO is transformed into an Ising model with the Hamiltonian consisting of a weighted sum of tensor products of Pauli Z operators. We use Z_i to denote both the spin variables, and the Pauli Z operators when clear from context. We may convert binary variables x_i into spin variables $Z_i \in \{-1, 1\}$ by $x_i = \frac{Z_i + 1}{2}$ and represent them in an Ising model of the following Hamiltonian

$$\mathcal{H} := \sum_{i=1} v_i Z_i + \sum_{j < i} J_{ij} Z_i Z_j + C \quad (2)$$

where J_{ij}, v_i encode the elements in the matrix Q . C is a constant offset which is typically ignored since it doesn't affect the optimal objective value. There is a one-to-one correspondence between the spin variables Z_i and the binary variables x_i . Once a problem is cast as a QUBO, it may be solved on an annealer. A quantum annealer works by exploiting quantum mechanical effects to find low energy states of the Hamiltonian in equation (2) [16]. The output of an annealer is non-deterministic, so it is sampled many times to obtain a representative distribution. Given M samples, the expected value of a variable Z_i is $\langle Z_i \rangle = \frac{\sum_m Z_i^m}{M}$, where m is the index of the sample.

III. PROBLEM FORMULATION

We are given a timetable of customers, each with a time window $[e_i, l_i]$, and a service time q_i ; an example is shown in Table I. The start of service must be within the time window. We start by discretizing time such that for each time window, there exists a time discretization $t \in [e_i, l_i]$. If an agent arrives at customer before e_i , we allow for waiting. We create variables $x_{i,s,j,t}$ representing "an agent leaves customer i at time s , and subsequently leaves customer j at time t ". We duplicate the depot to create original depot 0, and final depot N . The set T is the set of time discretizations, the set W is the set of customers, which excludes depots. For any variable $x_{i,s,j,t}$ we can compute $b_{ij} = \max\{e_j, s + d_{ij}\}$ where d_{ij} is the distance between customers i and j . b_{ij} is the earliest possible time we can start servicing customer j , having left customer i at time s . We use an arc-based formulation from [6]: the constrained binary optimization (QUBO) is shown in equation (3).

The objective is in (3a). Constraint (3b) ensures that all customers are visited. Constraint (3c) enforces flow between

consecutive customers. The remaining constraints are for pre-processing, and domain constraints.

$$\min_{x_{i,s,j,t}} \sum_{j \in W} \sum_t x_{0,0,j,t} \quad (3a)$$

$$\text{s.t.} \quad \sum_{i \in \{0,W\},s,t} x_{i,s,j,t} = 1, \quad \forall j \in W \quad (3b)$$

$$\sum_{j \in \{0,W\},j \neq i,t} x_{j,t,i,s} = \sum_{j \in \{W,N\},j \neq i,t} x_{i,s,j,t}, \quad \forall i \in W, \forall s \quad (3c)$$

$$x_{i,s,0,t} = 0, \quad \forall s, t, \quad \forall i \in \{0, W, N\} \quad (3d)$$

$$x_{N,s,j,t} = 0, \quad \forall s, t, \quad \forall j \in \{0, W, N\} \quad (3e)$$

$$x_{0,s,j,t} = 0, \quad \forall s \neq 0, \forall t, \quad \forall j \in \{0, W, N\} \quad (3f)$$

$$x_{i,s,j,t} = 0, \quad \forall i, s, t, \quad \forall j \in \{0, W, N\} : b_{ij} > l_j, \quad (3g)$$

$$x_{i,s,j,t} = 0, \quad \forall i, s, t, \quad \forall j \in \{0, W, N\} : t < b_{ij} + q_j \quad (3h)$$

$$x_{i,s,i,t} = 0, \quad \forall s, t, \quad \forall i \in \{0, W, N\} \quad (3i)$$

$$x_{i,0,j,t} = 0, \quad \forall i \neq 0, \forall t, \quad \forall j \in \{0, W, N\} \quad (3j)$$

$$x_{i,s,j,0} = 0, \quad \forall i, s, \quad \forall j \in \{0, W, N\} \quad (3k)$$

$$x_{0,s,N,t} = 0, \quad \forall s, t \quad (3l)$$

$$x_{i,s,j,t} \in \{0, 1\} \quad (3m)$$

A. Pre-processing

Our formulation initially may appear to have a formidable number of variables. However, by making a few observations, we are able to prune many of the variables by fixing their values to 0, and removing them from the model. The variables we can prune correspond to constraints (3d)-(3l), and are described in Table II.

TABLE II: Constraint and Description for Pre-processing variables in problem (3)

| Constraint | Description |
|------------|--|
| (3d) | Cannot enter original depot |
| (3e) | Cannot leave final depot |
| (3f) | Can only leave original depot at time 0 |
| (3g) | Cannot be late to service customer j |
| (3h) | Cannot leave customer j before end of service time |
| (3i) | No self-loops |
| (3j) | Cannot leave customers at time 0 |
| (3k) | Cannot leave any nodes at time 0, after node i |
| (3l) | Cannot travel immediately from original depot to final depot |

IV. METHODS

A. Greedy Quantum Route-Finding Algorithm

Our algorithm for solving problem (3) is shown in Algorithm 1. We first observe that any subset of the variables in our formulation can be represented as a directed acyclic graph. By combining this with the samples obtained from the annealer, we can converge quickly to a feasible solution. The main idea, is the following: the annealer recommends a set of variables to be used in constructing a DAG, and a classical routine is used to find feasible sub-paths within the DAG. The variables

corresponding to customers along each of the paths are pruned. Variables that haven't been pruned are still "active". At each iteration the set of active variables X , gets smaller, while the cumulative set of feasible paths returned S , gets larger. The algorithm terminates when $X^l = \emptyset$, although in practice may be terminated when the number of active variables is small enough to solve the problem exactly.

We use Q to denote the new set of edge-and-vertex-disjoint paths found in the DAG, and P to denote a single path in Q . Paths consist of a sequence of tuples $\{(i_k^P, s_k)\}_{k=0}^{|P|}$. We use i_k^P to denote the customer at index k of path P , and no superscript is used when clear from context. Let X^l denote the set of variables "active" at iteration l , S^l denote the cumulative set of paths found in iterations prior to l , and Q^l the set of paths found at iteration l . We use (3b, i) to denote the coverage constraints for customer i , and (3c, i, s) to denote the flow constraints for customer i at timestep s . $\text{DAG}(X)$ denotes the DAG formed by the variables in set X . $\text{QUBO}(X)$ denotes solving problem (3) using annealing, over the set of variables X . \mathcal{X} denotes the samples returned by the annealer. A, M are annealing time and number of samples, resp. They are implicitly inputs to $\text{QUBO}(X)$. When clear from context, i is the index of a single variable in X^l . We use $R \frown R'$ to denote the concatenation of two paths R and R' . The final set of paths returned as a solution to the FSVRPTW (3) is S . Step 6 computes a statistic used in step 7

Algorithm 1 Greedy Quantum Route-Finding Algorithm

Input: $X^0 = \{x_{i,s,j,t}\}$ initially, all variables "active", θ, M , number of annealing samples, A , annealing time.

Output: S , paths found

```

1:  $S^0 \leftarrow \emptyset$ 
2: while  $X^l \neq \emptyset$  do
3:    $\mathcal{X}^l \leftarrow \text{QUBO}(X^l)$ 
4:   for  $i \in 1 \dots |X^l|$  do
5:     Compute  $| \langle Z_i \rangle |$  over all  $M$  samples
6:   end for
7:    $\bar{X}^l \leftarrow$  Select  $\theta$  % of  $X^l$  with highest  $| \langle Z_i \rangle |$ 
8:    $Q^l \leftarrow$  Find paths in  $\text{DAG}(\bar{X}^l)$ 
9:    $S^{l+1}, X^{l+1} \leftarrow \text{PRUNE}(S^l, X^l, Q^l)$ 
10: end while

```

to determine which variables will participate in the DAG for finding paths. In our algorithm, we used one-body expectation values $| \langle Z_i \rangle |$, although two-body expectation values may be used [12]. Parameter $\theta \in (0, 1)$ is given by the user to determine the variables in X^l to select at each iteration. θ may be given as a portion of the variables to select, or as a threshold for expectation values. In our running example and our analysis, we specify θ as a portion, although the results still hold for θ as a threshold. For step 8, any subroutine may be used that guarantees that no 2 paths returned visit same customer. This ensures that the paths are edge-and-vertex-disjoint. Two examples are: returning the longest path, or returning multiple paths. Multiple paths may be returned by an iterative procedure: 1. Select the longest path in the DAG.

2. Remove all nodes (and their adjacent edges) in the DAG with the same customers i_k (excluding depots $0, N$) along the currently-selected longest path, 3. Remove the nodes and arcs along the currently-selected longest path from the DAG. Repeat until the DAG is empty. In the simulation results, we returned multiple paths using this procedure. Heuristics such as returning a single longest path are more conservative, and may lead to longer computational time since fewer variables would be fixed at each iteration.

B. DAG Representation

We now describe the construction of the DAG. Any set of active variables X^l may be represented as follows: A single node is created for each unique tuple (i, s) , where $i \in \{0, W, N\}$ and $s \in T$. A directed arc is present from (i, s) to (j, t) for each variable $x_{i,s,j,t} \in X^l$. By constraints (3g) and (3h), after the pre-processing described in section III-A variables only remain active if $s < t$. There cannot exist a cycle, otherwise it would imply that there exists a variable $x_{i,s,j,t}$ such that $s \geq t$. $\text{DAG}(X^0)$ for our running example is shown in Fig. 1.

C. Pruning

The subroutine $\text{PRUNE}(S, X, Q)$ is shown in Algorithm 2. Notice that the constraints (3b) and (3c) are separable by customer j , and tuples (i, s) respectively. So we may prune variables and remove constraints independently for each tuple (i, s) , along a path in steps 4, 6, and 9 in Algorithm 2. If a path is found that shares an endpoint (either start or end) of a path in S , the paths are concatenated by CONCAT and the appropriate constraints are removed, as shown in Algorithm 3.

Algorithm 2 Prune

Input: S , set of paths found previously, Q , new set of paths found, X , current set of active variables.

Output: S' , new set of paths found, X' , new set of active variables, QUBO', new problem (3) formulation

```

1: for  $P \in Q$  do
2:   QUBO  $\leftarrow$  CONCAT( $S, P, \text{QUBO}$ )
3:   for  $(i_k, s_k) \in P$  do
4:      $X' \leftarrow$  Apply pruning rules in section IV-C1.
5:     if  $k \notin \{0, |P|\}$  then
6:       QUBO  $\leftarrow$  remove constraint (3c,  $i_k, s_k$ )
7:     end if
8:     if  $k \neq 0$  then
9:       QUBO  $\leftarrow$  remove constraint (3b,  $i_k$ )
10:    end if
11:  end for
12: end for

```

Algorithm 3 Concat

Input: S, P, QUBO

Output: QUBO', S

```

1: for  $P' \in S$  do
2:   if  $i_0^P = i_{|P'|}^{P'}$  for  $(i_0^P, s) \in P$  then
3:      $P' \leftarrow P' \cup P$ 
4:     QUBO  $\leftarrow$  Remove constraints (3c,  $i_0^P, s$ )
5:   end if
6:   if  $i_{|P|}^P = i_0^{P'}$  for  $(i_{|P|}^P, s) \in P$  then
7:      $P' \leftarrow P \cup P'$ 
8:     QUBO  $\leftarrow$  Remove constraints (3c,  $i_{|P|}^P, s$ ), (3b,  $i_{|P|}^P$ )
9:   end if
10: end for

```

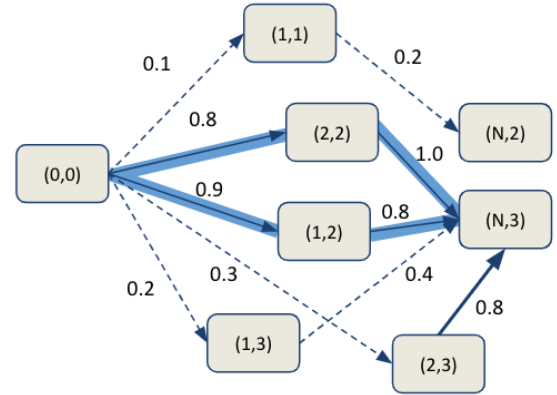


Fig. 1: Initial set of variables X^0 represented as a DAG (denoted $\text{DAG}(X^0)$), continued from example in Tab. I, labeled with possible one-body expectation values from step 6 in Algorithm 1. Variables selected in step 7 in Algorithm 1, using $\theta = 0.5$ are marked with solid arrows. Paths found in step 8 in Algorithm 1 are highlighted in blue.

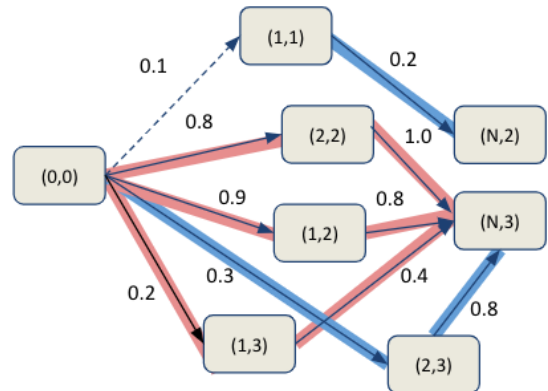


Fig. 2: Pruning example for $\theta = 0.9$. Arcs in paths found in step 8 of Algorithm 1 are highlighted blue, and variables along the path are set to 1 and pruned. Arcs highlighted red are set to 0 and pruned. Paths found are $P_1 = \{(1,1), (N,2)\}$, $P_2 = \{(0,0), (2,3), (N,3)\}$.

TABLE III: Pruning Rules Applied to Fig. 2

| Path | k | (i_k, s_k) | Variables Pruned | Pruning Rule | | |
|-------|-----|--------------|-------------------|--------------|-------------------|-------------|
| P_1 | 0 | (1, 1) | $x_{1,1,N,2} = 1$ | Along path | | |
| | | | $x_{0,0,1,2} = 0$ | exterior 1b | | |
| | | | $x_{0,0,1,3} = 0$ | exterior 1b | | |
| | | | $x_{1,3,N,3} = 0$ | exterior 1b | | |
| | | | $x_{1,2,N,3} = 0$ | exterior 1b | | |
| | 1 | (N, 2) | None | exterior 2a | | |
| P_2 | 0 | (0, 0) | $x_{0,0,2,3} = 1$ | Along path | | |
| | | | 1 | (2, 3) | $x_{2,3,N,3} = 1$ | Along path |
| | | | 2 | (N, 3) | $x_{0,0,2,2} = 0$ | interior 2a |
| | | | $x_{2,2,N,3} = 0$ | interior 1a | | |

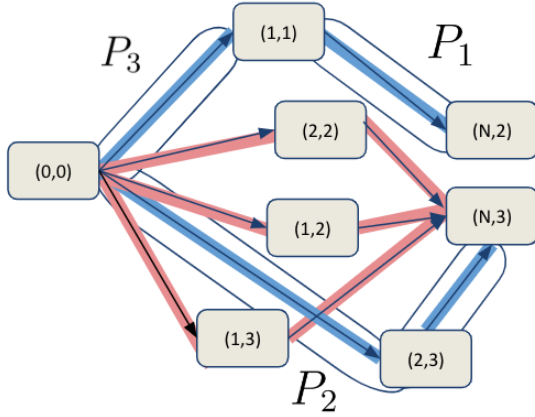


Fig. 3: Subsequent iteration for pruning example with $\theta = 0.9$. (Expectation values omitted to avoid clutter). After pruning in previous iteration, only variable $x_{0,0,1,1}$ remains active. Path $P_3 = \{(0,0), (1,1)\}$ is found in step 8 of Algorithm 1, and joined with path P_1 in step 7 of Algorithm 3.

1) *Pruning Rules:* Throughout this section, the phrase "prune" means the variable is set to the value specified and removed from the set of active variables X^l . For customer i_k of tuple (i_k, s_k) , variables involving customer i_k may be classified as:

- 1) $i = i_k$: "outgoing" variables.
- 2) $j = i_k$: "incoming" variables.

Index $k \in 0, \dots, |P|$ along a path P may be classified

- 1) $k \notin \{0, |P|\}$: "interior" indices.
- 2) $k \in \{0, |P|\}$: "exterior" indices.

Using this terminology we iterate over tuples (i_k, s_k) and prune by the following rules:

Along path: If variable $x_{i_k, s_k, i_{k+1}, s_{k+1}}$ is an arc along the path for two consecutive tuples $(i_k, s_k), (i_{k+1}, s_{k+1})$, it is set to 1 and pruned.

If k is "interior":

- 1) "outgoing" variables are set to 0 and pruned if either:
 - a) $i = i_k$ and $s \neq s_k$ OR
 - b) $i = i_k$, and $s = s_k$, and either:
 - i) $j \neq i_{k+1}$ OR

ii) $t \neq s_{k+1}$

- 2) "incoming" variables are set to 0 and pruned if either:
 - a) $j = i_k$ and $t \neq s_k$ OR
 - b) $j = i_k$, and $t = s_k$, and either:
 - i) $i \neq i_{k-1}$ OR
 - ii) $t \neq s_{k-1}$

If k is "exterior":

- 1) $k = 0$:
 - a) $i_k = 0$: Only prune and set = 1 if $x_{i_k, s_k, i_{k+1}, s_{k+1}}$ is **Along path**. (Variables incoming to depot were pruned by (3d)).
 - b) $i_k \neq 0$: Prune using rules "interior" 1 and 2a.
- 2) $k = |P|$:
 - a) $i_k = N$: Prune using "interior-incoming" 2a. (We do not prune according to rules 2b because incoming arcs to final depot N at different times is allowed, as shown in Fig. 1).
 - b) $i_k \neq N$: Prune incoming variables under interior rule 2, and outgoing variables under interior rule 1a.

V. ANALYSIS

Lemma 1. In any iteration l , if a customer i_k^P is in the interior of path $P \in S^l$, all outgoing and incoming variables to that customer have been pruned.

Proof. Assume without loss of generality that P was formed by the union of paths R and R' , found at iterations l^R and $l^{R'}$, respectively. $P = R \cap R'$. For customer i_k^P there are two cases:

- 1) i_k^P was in the interior of either path R or R' . So it was either pruned to 1 by the "Along path" rules, or pruned to 0 by the "interior" rules in section IV-C.
- 2) i_k^P was in the exterior of either path R or R' . The incoming variables to i_k^P were pruned in iteration l^R by "exterior" rule 2b and the outgoing variables were pruned in iteration $l^{R'}$ by "exterior" rule 1b. □

Lemma 2. For every customer i' , \exists iteration l' in which the paths $Q^{l'}$ returned in step 8 of Algorithm 1 will contain a path with a tuple (i', s) for some s .

Proof. Every set of samples returned from the annealer \mathcal{X}^l in iteration l there are 2 cases:

- 1) Annealer returns 0 for all variables, for all samples. Then no variables are pruned, and the while loop resumes.
- 2) There exists a sample $\mathcal{X}_m^l \in \mathcal{X}^l$ with at least one variable $x_{i,s,j,t} = 1$. Then at least one variable will be in \bar{X}^l since $\theta \in (0, 1)$. Then there are two cases:
 - a) \bar{X}^l does not contain a variable $x_{i,s,j,t}$ with either $i' = i$ or $i' = j$. Variables containing customers along paths returned by step 8 will be pruned according to the pruning rules in section IV-C1, and the while loop resumes its next iteration with $X^{l+1} \subset X^l$.
 - b) \bar{X}^l contains a variable $x_{i,s,j,t}$ with either $i' = i$ or $i' = j$. Then there are two cases:

- i) The paths returned by step 8 contain a tuple (i', s) for some s .
- ii) They do not.

In case 2(b)ii the variables containing customers along paths returned by step 8 will be pruned according to the pruning rules in section IV-C1, and the while loop resumes its next iteration with $X^{l+1} \subset X^l$. If in case 2(b)i. QED. If the annealing time A is sufficiently large, [17] eventually we will exit case 1. If we continue to be in cases 2a or 2(b)ii above, then paths returned in step 8 in Algorithm 1 do not contain tuple (i', s) , and in the next iteration $X^{l+1} \subset X^l$. By Lemma 1, all variables in the interior of previously-found paths S will be pruned. At some iteration l' the only variables not pruned are those containing tuple (i', s) , in which case they must appear in the paths returned in step 8. \square

Lemma 3. *If customer i_k^R was in the exterior of path $R \in Q^l$ in iteration l , then it will be in the interior of some path $P \in S^{l'}$ for an iteration $l' > l$.*

Proof. If $k = 0$ then all outgoing variables and incoming variables to i_0^R with $t \neq s_0^R$ have been pruned in "exterior" rule 1b. So, the only active variables involving i_0^R have $(j, t) = (i_0^R, s_0^R)$. By Lemma 2, in iteration l' path $R' \in Q^{l'}$ will contain (i_0^R, s_0^R) . This can only happen if $i_{|R'|}^{R'} = i_0^R$. In step 7 in Algorithm 3 these paths are unioned, and the resulting path $P = R' \cup R$ will have i_0^R in its interior.

The proof for $k = |R|$ is the similar, except $i_0^R = i_{|R|}^R$, and the resulting path is $P = R \cup R'$. \square

Lemma 4. *Algorithm 1 converges to a feasible solution to Problem (3).*

Proof. Observe that all variables contain a customer by preprocessing constraint (31). By Lemma 3 at some iteration, any customer i will be in the interior of some path $P \in S$. By the pruning rules, when a customer is in the interior of a path $P \in S$ we have set exactly two variables involving customer i equal to 1: one incoming, and one outgoing. All other variables involving customer i have been pruned and set to 0. Thus constraint (3b) is satisfied. By the same argument, if (i, s) is along a path in S returned by Algorithm 1 then exactly one variable on each side of constraint (3c, i, s) will be 1 - all others have been pruned by rules "interior" 1 and 2. If (i, s) is not along a path, then constraints (3c, i, s) will become $0 = 0$ and will be satisfied again by rules "interior" 1 and 2. Since constraints (3b) and (3c) are satisfied the paths S returned by Algorithm 1 are a feasible solution to Problem (3). \square

VI. COMPUTATIONAL RESULTS

A. Solvers

We benchmark with both classical and quantum annealing approaches that attempt to find a feasible solution to the FSVRPTW. In the absence of obvious heuristics for restoring feasibility, the standard approach is to run quantum annealer to obtain a distribution of samples, and select the feasible sample with the lowest energy. We give a brief description

TABLE IV: QPU Results

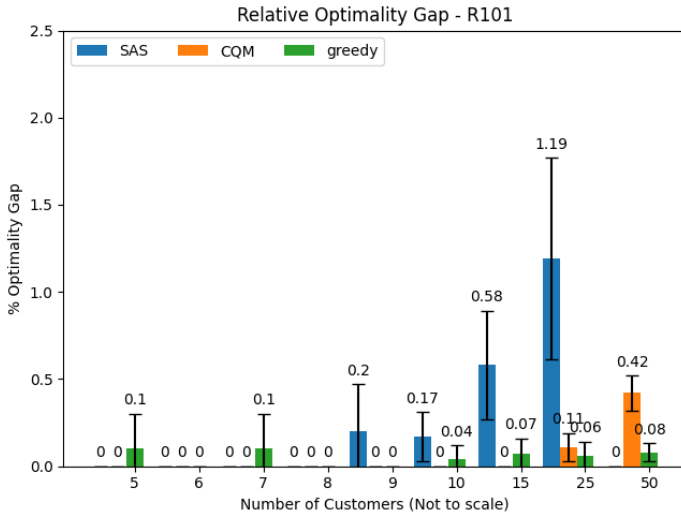
| N | DWaveSampler ($A = 50\mu s$, $M = 2000$) % Valid | DWaveSampler ($A = 50\mu s$, $M = 2000$) with Pause % Valid | t_{greedy} | α | Avg. # log- ical | Avg. # phys- ical |
|-----|--|--|---------------------|----------|---------------------------|----------------------------|
| 5 | 20 | 10 | 0.08 | 10 | 44 | 415 |
| 6 | 0 | 0 | 0.074 | 17 | 84 | 601 |
| 7 | 0 | 0 | 0.08 | 33 | 109 | 890 |
| 8 | 0 | 0 | 0.09 | 0 | 121 | 955 |
| 9 | 0 | 0 | 0.09 | 0 | 127 | 1021 |

of each method used: Simulated annealing (SAS) is a classical metaheuristic algorithm that mimicks the physical process of annealing. Its algorithmic parameters include an annealing schedule. We use the `SimulatedAnnealingSampler` (SAS) provided by D-Wave, and we use the default settings of a geometric schedule [18]. LeapHybridCQMSampler (CQM) is a hybrid classical/quantum annealer that is specifically designed to solve problems with constraints. Its algorithmic parameters include `num_reads`, which is the number of samples returned by the annealer. The more samples, the greater chance of finding a solution with low energy. We used D-Wave's CQM version 1p solver, and set `num_reads=1000`. In our greedy algorithm we used CQM for solving the QUBO(X) in step 1, with the default parameters, and the default penalty values. To evaluate the performance of our proposed algorithm for practical-sized problems we used Solomon's benchmark instances [19], briefly described as graphs with nodes that must be serviced with a time window, placed according to a random distribution. We used instance types $R101/R201$ which indicates narrow/wide time windows resp. We modify an instance to suit our problem as follows: for a given number of customers, randomly sample N customers. For each value of N , we construct 10 random examples independently, and aggregate their statistics.

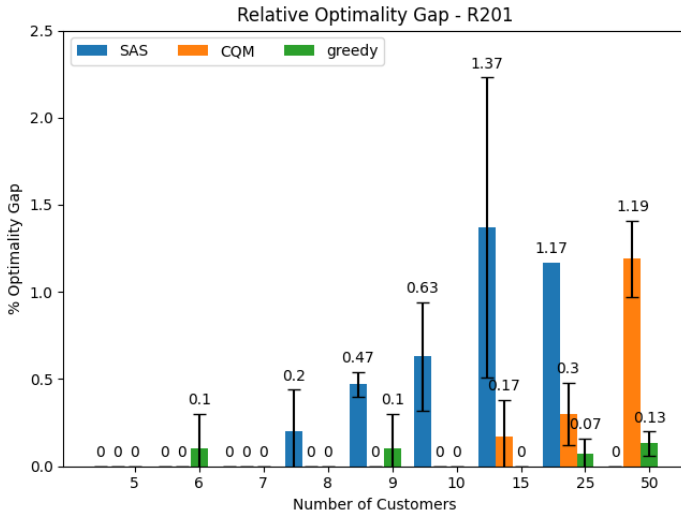
From Fig. 4a, and 4b we can see that our greedy approach enjoys a small relative optimality gap as compared to SAS and CQM, in particular for large problem sizes $N > 15$. This difference is even more pronounced in the R201 examples. For $N = 25$, SAS returned feasible solutions for only 2 of the 10 random examples, and for $N = 50$ it returned no feasible solutions. Statistics are aggregated only over feasible solutions. Fig. 5a, and 5b show the relative time difference between the greedy algorithm, and CQM/SAS. Positive values indicate greedy algorithm is faster. For large problem instances greedy is always faster than SAS, although CQM is faster by a small margin for $N > 15$.

VII. QPU RESULTS

To evaluate its robustness to noise, our algorithm was also tested on DWave Advantage 4.1. For a fair benchmark, we also tried tuning the parameters of the `DWaveSampler`. An annealing pause was used by setting it to: $[0.0, 0.0]$, $[10.0, 0.4]$, $[50.0, 0.4]$, $[120, 1.0]$. Annealing pauses are showing to perform well



(a) Solomon R101 Examples

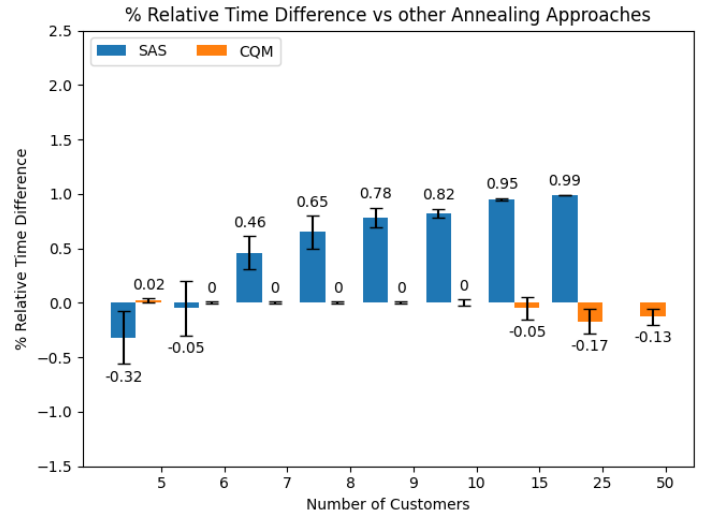


(b) Solomon R201 Examples

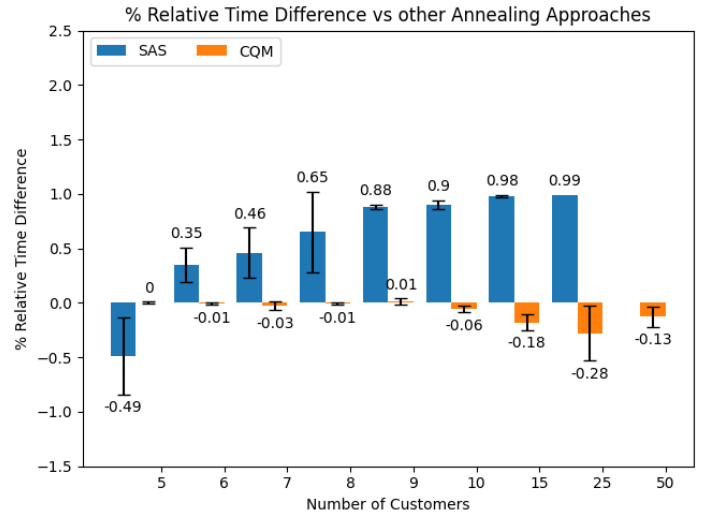
Fig. 4: Average relative optimality gap for SAS, CQM, and the proposed greedy algorithm, averaged over 10 examples with standard deviation. Relative optimal value is computed as $\frac{C_A - C_{opt}}{C_{opt}}$ where C_A is the objective value found by the annealing method, and C_{opt} is the optimal value found by Gurobi version 10.0.3. Statistics are computed only over feasible solutions. Data not shown for SAS, $N = 50$, because no feasible solutions were found.

for scheduling problems [20]. Finally, to increase the chance of the DWaveSampler finding a feasible solution, both the annealing time, and the number of samples were adjusted to $50\mu s$ and $M = 2000$, respectively. (This is the largest these values can be increased before the DWave’s QPU access time is exceeded [21]). In our greedy algorithm, we left the annealing parameters in DWaveSampler to their default values.

Our experiments revealed that even after enhancing the DWaveSampler with these features, it fails to find any



(a) Solomon R101 Examples



(b) Solomon R201 Examples

Fig. 5: Average relative time difference of greedy as compared to SAS and CQM averaged over 10 examples. Relative time difference is computed as $\frac{t_A - t_{greedy}}{t_A}$ where t_A is the time taken by the annealing method, and t_{greedy} is the time taken by our proposed greedy algorithm. Statistics are computed only over feasible solutions. Data not shown for SAS, $N = 50$, because no feasible solutions were found.

feasible solutions in any of the 10 examples for problem sizes greater than $N=5$ customers. The greedy algorithm, when using the default DWaveSampler parameters, still maintains an average relative optimality gap below 33%. The total time of Algorithm 1, and the average relative optimality gap are labeled t_{greedy} , and α , respectively, Table IV.

To show the scaling of this formulation on the binary variables, the average number of logical qubits and physical qubits are also reported. When the number of customers exceeds 7, the rate at which the number of logical qubits increases more slowly. This can be explained by the fact

that only one discretization value within each time window is needed. If there is already one time discretization within a time window, then we avoid creating a new one. As a timetable includes more customers, more of the time windows overlap.

CONCLUSIONS AND FUTURE WORK

This work presents the first effective algorithm for generating routes using an annealing-based approach. We demonstrated its efficiency by solving the FSVRPTW. We prove that it converges to a feasible solution, and we benchmark it against state-of-the-art classical and hybrid annealing-based approaches using D-Wave. We showed it enjoys a smaller optimality gap than other annealing-based approaches, at a competitive computation time, even for practical-sized problems of 50 customers. It also shows to be noise-robust when executed on a QPU, by taking advantage of the entire sample set returned by the annealer. Natural directions for future work include determining the dependence of the proposed algorithm's performance on the dataset, e.g. using different time discretizations and graphs generated from different distributions. We may also explore the effect of the control parameters, e.g. θ . These future directions will provide insight into how this adaptive algorithm may be used to solve a more general class of problems outside of routing and scheduling.

VIII. ACKNOWLEDGEMENTS

J.M. acknowledges Ketan Savla, and David E. Bernal Neira for helpful input and discussion during the development of these ideas.

REFERENCES

- [1] Sebastian Feld, Christoph Roch, Thomas Gabor, Christian Seidel, Florian Neukart, Isabella Galter, Wolfgang Mauerer, and Claudia Linnhoff-Popien. A hybrid solution method for the capacitated vehicle routing problem using a quantum annealer. *Frontiers in ICT*, 6:13, 2019.
- [2] Eneko Osaba, Esther Villar-Rodríguez, and Izaskun Oregi. A systematic literature review of quantum computing for routing problems. *IEEE Access*, 10:55805–55817, 2022.
- [3] Özlem Salehi, Adam Glos, and Jarosław Adam Miszczak. Unconstrained binary models of the travelling salesman problem variants for quantum optimization. *Quantum Information Processing*, 21(2):67, 2022.
- [4] Christos Papalitsas, Theodore Andronikos, Konstantinos Giannakis, Georgia Theocharopoulou, and Sofia Fanarioti. A qubo model for the traveling salesman problem with time windows. *Algorithms*, 12(11):224, 2019.
- [5] Hirotaka Irie, Goragot Wongpaisamsin, Masayoshi Terabe, Akira Miki, and Shinichirou Taguchi. Quantum annealing of vehicle routing problem with time, state and capacity. In *Quantum Technology and Optimization Problems: First International Workshop, QTOP 2019, Munich, Germany, March 18, 2019, Proceedings 1*, pages 145–156. Springer, 2019.
- [6] Stuart Harwood, Claudio Gambella, Dimitar Trenev, Andrea Simonetto, David Bernal, and Donny Greenberg. Formulating and solving routing problems on quantum computers. *IEEE Transactions on Quantum Engineering*, 2:1–17, 2021.
- [7] Hanjing Xu, Hayato Ushijima-Mwesigwa, and Indradeep Ghosh. Scaling vehicle routing problem solvers with qubo-based specialized hardware. In *2022 IEEE/ACM 7th Symposium on Edge Computing (SEC)*, pages 381–386. IEEE, 2022.
- [8] Lilly Palackal, Benedikt Poggel, Matthias Wulff, Hans Ehm, Jeanette Miriam Lorenz, and Christian B Mendl. Quantum-assisted solution paths for the capacitated vehicle routing problem. In *2023 IEEE International Conference on Quantum Computing and Engineering (QCE)*, volume 1, pages 648–658. IEEE, 2023.
- [9] Dimitris Angelakis. Qubit efficient quantum algorithms for the vehicle routing problem on nisq processors. *Bulletin of the American Physical Society*, 2024.
- [10] David E Bernal Neira, Carl D Laird, Laurens R Lueg, Stuart M Harwood, Dimitar Trenev, and Davide Venturelli. Utilizing modern computer architectures to solve mathematical optimization problems: A survey. *Computers & Chemical Engineering*, page 108627, 2024.
- [11] Ramin Ayanzadeh, John Dorband, Milton Halem, and Tim Finin. Quantum-assisted greedy algorithms. In *IGARSS 2022-2022 IEEE International Geoscience and Remote Sensing Symposium*, pages 4911–4914. IEEE, 2022.
- [12] Maxime Dupont, Bram Evert, Mark J Hodson, Bhuvanesh Sundar, Stephen Jeffrey, Yuki Yamaguchi, Dennis Feng, Filip B Maciejewski, Stuart Hadfield, M Sohaib Alam, et al. Quantum-enhanced greedy combinatorial optimization solver. *Science Advances*, 9(45):ead0487, 2023.
- [13] Maxime Dupont and Bhuvanesh Sundar. Extending relax-and-round combinatorial optimization solvers with quantum correlations. *Physical Review A*, 109(1):012429, 2024.
- [14] J. A. Montanez-Barrera, Pim van den Heuvel, Dennis Willsch, and Kristel Michiels. Improving performance in combinatorial optimization problems with inequality constraints: An evaluation of the unbalanced penalization method on d-wave advantage, 2023.
- [15] John Preskill. Quantum computing in the nisq era and beyond. *Quantum*, 2:79, August 2018.
- [16] Satoshi Morita and Hidetoshi Nishimori. Mathematical foundation of quantum annealing. *Journal of Mathematical Physics*, 49(12), 2008.
- [17] Tameem Albash and Daniel A Lidar. Adiabatic quantum computation. *Reviews of Modern Physics*, 90(1):015002, 2018.
- [18] dwave-neal 2014; dwave-neal 0.5.9 documentation — docs.ocean.dwavesys.com. <https://docs.ocean.dwavesys.com/projects/neal>. [Accessed 26-04-2024].
- [19] Marius M Solomon. Algorithms for the vehicle routing and scheduling problems with time window constraints. *Operations research*, 35(2):254–265, 1987.
- [20] Jeffrey Marshall, Davide Venturelli, Itay Hen, and Eleanor G Rieffel. Power of pausing: Advancing understanding of thermalization in experimental quantum annealers. *Physical Review Applied*, 11(4):044083, 2019.
- [21] Ocean Documentation 6.10.0 documentation. https://docs.ocean.dwavesys.com/en/stable/docs_cloud/reference/generated/dwave.cloud.solver.StructuredSolver.estimate_qpu_access_time.html. [Accessed 01-05-2024].